ELSEVIER

Contents lists available at ScienceDirect

# Journal of Neuroscience Methods

journal homepage: www.elsevier.com/locate/jneumeth





# Determining the optimal expression method for dual-color imaging

Jacob F. Norman\*, Bahar Rahsepar, Jad Noueihed, John A. White

Dept. of Biomedical Engineering, Center for Systems Neuroscience, Neurophotonics Center, Boston University, Boston, MA, 02215, United States

ARTICLE INFO

Keywords: Calcium imaging GCaMP Cell-type specificity

#### ABSTRACT

*Background:* Fluorescence imaging is a widely used technique that permits for cell-type-specific recording from hundreds of neurons simultaneously. Often, to obtain cell-type-specific recordings from more than one cell type, researchers add an additional fluorescent protein to mark a second neuronal subpopulation. Currently, however, no consensus exists on the best expression method for multiple fluorescent proteins.

New Method: We optimized the coexpression of two fluorescent proteins across multiple brain regions and mouse lines

*Results:* The single-virus method, a viral injection in a double transgenic reporter mouse, results in limited fluorescent coexpression. In contrast the double-virus method, injecting a mixture of two viruses in a Cre driver mouse, results in up to 70 % coexpression of the fluorescent markers *in vitro*. Using the double-virus method allows for population activity recording and neuronal subpopulation determination.

Comparison with Existing Method: The standard for expressing two fluorescent proteins is to use a double transgenic reporter mouse with a single viral injection. Injecting two viruses into a Cre driver mouse resulted in significantly higher coexpression compared to the standard method. This result generalized to multiple brain regions and mouse lines in vitro, as well as in vivo.

*Conclusion:* Efficiently coexpressing multiple fluorescent proteins provides population activity while identifying a neuronal subpopulation of interest. The improved coexpression is applicable to a wide breadth of experiments, ranging from engram investigation to voltage imaging.

# 1. Introduction

The mammalian brain is comprised of a diverse population of neurons, which together form neural circuits enabling cognitive function. Different types of neurons exist within small spatial volumes, each with unique morphology, electrophysiology, and connectivity (Zeng and Sanes, 2017; Luo et al., 2018). Individual subpopulations across various brain regions have been shown to play specific computational roles and are implicated in numerous disease states (Hnasko et al., 2012; Tan et al., 2012; Urban-Ciecko and Barth, 2016; Ferguson and Gao, 2018; Adler et al., 2019; Surmeier, 2018). Diseases such as major depression and schizophrenia are linked to dysregulation of excitation and inhibition, which are mediated by distinct classes of neurons (Benes and Berretta, 2001; Gao and Penzes, 2015; Fogaça and Duman, 2019). While the properties of single excitatory and inhibitory neurons have been established, how these neurons interact to perform computations remains unclear. Furthermore, the set of inhibitory neurons is not homogeneous. For example, parvalbumin-positive (PV) interneurons are generally fast firing and provide direct inhibition to cell bodies, while somatostatin-positive (SOM) interneurons generally project to pyramidal cell dendrites and other inhibitory neurons (Hertäg and Sprekeler, 2019; Swanson and Maffei, 2019). Understanding the dynamics and interactions of different classes of neurons in local circuits is crucial for unraveling neuronal processing in the brain and elucidating mechanisms underlying neurological disease states.

Molecular biology provides tools to distinguish and record from subpopulations of neurons based on their genetic profile. The Cre-Lox system leverages cell-type-specific genes to restrict expression of exogenous genetic material to a desired set of neurons (Sauer, 1998; Gong et al., 2007; Feil et al., 2009). A distinct neuronal subpopulation can be marked fluorescently, providing anatomical and physiological data. These investigations have aided researchers in unraveling the network dynamics of specific neuronal subpopulations, including ocean and island cells in the medial entorhinal cortex (Kitamura et al., 2014, 2015) and mossy cells in the dentate gyrus (Danielson et al., 2017). Although imaging subpopulations allows for characterization of the specific cell

E-mail address: jfnorman@bu.edu (J.F. Norman).

<sup>\*</sup> Corresponding author.

type, it ignores the relationship between the cell type of interest and the population.

In order to identify network -cell type interactions, researchers incorporate multiple fluorophores. Typically, a static fluorophore is used to mark the cell type of interest, while a spectrally distinct dynamic fluorophore provides population activity data. Early dual-color imaging studies combined a fluorescent dye with a genetically encoded activity indicator (Marvin et al., 2013; Tischbirek et al., 2017), while more recent imaging studies commonly use genetically encoded fluorophores for both colors. Three methods exist to genetically express two fluorophores: 1) a triple transgenic mouse line, 2) a single viral injection into a double transgenic reporter mouse line, and 3) an injection of two viruses into a Cre driver mouse line. Creation of triple transgenic mice involves complex experimental techniques such as pronuclear injection and requires extensive validation (Ittner and Götz, 2007; Dougherty et al., 2012). Because of the experimental challenges, triple transgenic mice are not widely used and will not be considered in this work. A single viral injection into a double transgenic reporter mouse is the most common form of expressing two fluorophores because reporter mice are easy to obtain and viral injections are experimentally straightforward (Peron et al., 2015; Hayashi et al., 2018; Garcia-junco-clemente et al., 2019; Najafi et al., 2020; Tran et al., 2020). While a single viral injection into a reporter mouse adequately expresses both fluorophores, oftentimes the fluorophores are observed in distinct sets of cells with minimal overlap. An injection of two viruses into a Cre driver mouse is also experimentally straightforward, though it has been used less frequently (Gritton et al., 2019; Engelhard et al., 2020). Despite using longstanding experimental techniques, the latter two methods have not been directly compared.

In this work, we quantitatively investigate the methods for expressing two genetically encoded fluorophores *in vitro* and *in vivo*. We compare the methods across mouse lines and brain regions. Our *in vitro* and *in vivo* results indicate that expressing both fluorophores virally yields optimal coexpression.

### 2. Results

# 2.1. tdTomato expression in Gad2-Cre mice is insensitive to injection volume

Prior to investigating the expression of multiple fluorophores, we first optimized the expression of a single fluorophore. Gad2-Cre mice were injected with Flex-tdTomato in the somatosensory cortex. In mouse cortex, Gad2 is expressed exclusively in GABAergic cells. Although astrocytes have been reported to express Gad2 in the brainstem and the cerebellum, Gad2 positive astrocytes have not been observed in the mouse cortex (Ishibashi et al., 2019). Additionally, the morphology of the observed cells matches that of inhibitory neurons. The cortex was selected because labeled cells were sparse enough to accurately quantify while numerous enough to provide population estimates. A threefold

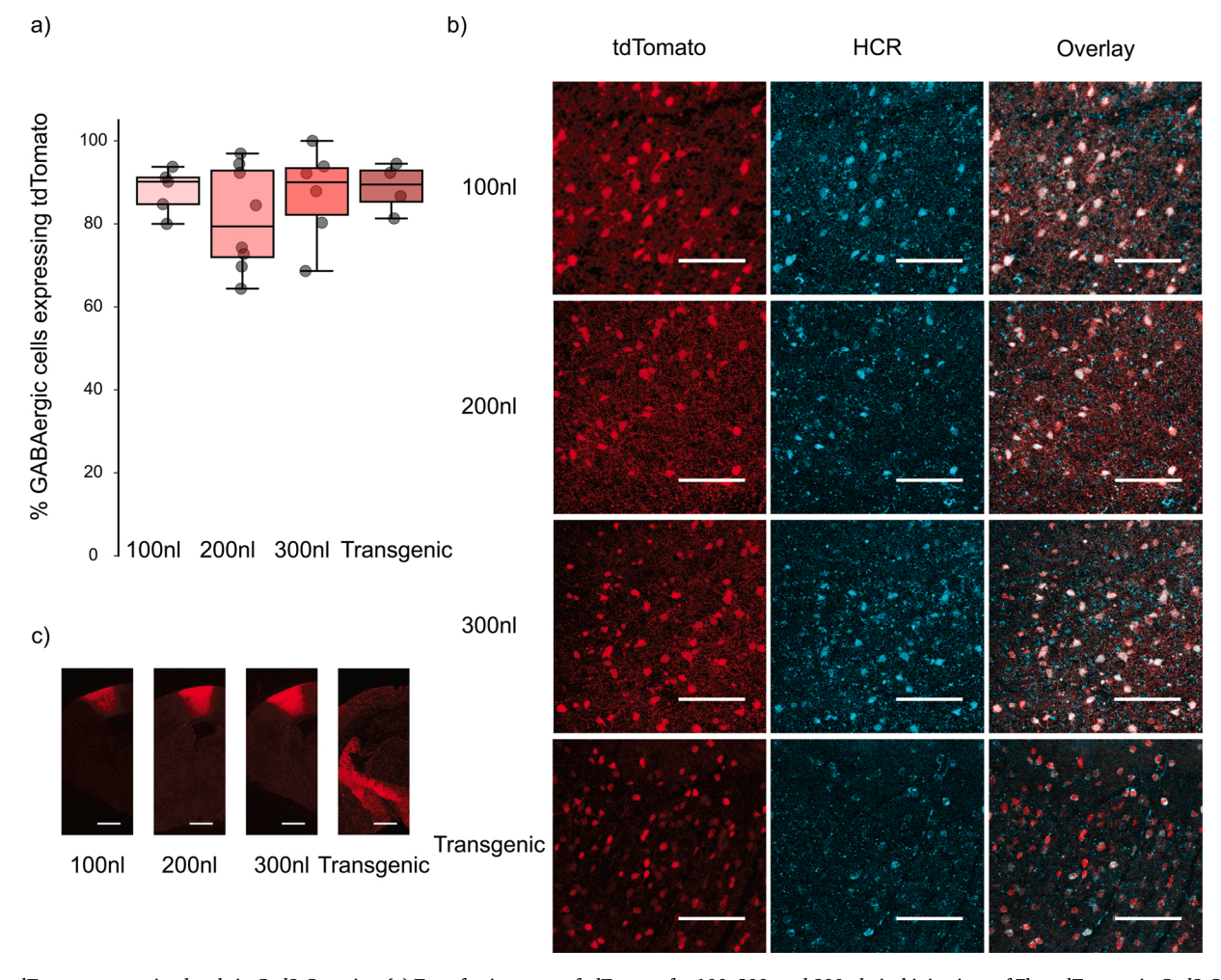


Fig. 1. tdTomato expression levels in Gad2-Cre mice. (a) Transfection rates of tdTomato for 100, 200, and 300 nl viral injections of Flex-tdTomato in Gad2-Cre mice, as well as double transgenic Gad2-Cre:LSL-tdTomato mice (n = 5, 7, 6, and 4 for 100 nl, 300 nl, and double transgenic, respectively. p = .76, Kruskal-Wallis H Test). (b) Overlays show HCR staining of Gad2 in blue and tdTomato in red. All samples are taken from the somatosensory cortex. Scale bars: 100  $\mu$ m. (c) Representative images showing the transfected regions in the injected mice. Scale bars: 1 mm.

range of injection volumes was tested. All sample groups had medians between  $\sim 80-90$  %, with none of the injection volumes resulting in a significantly different percentage of GABAergic cells expressing tdTomato. (Fig. 1a).

# 2.2. A single viral injection has similar expression to that of a double transgenic reporter mouse

After determining that our range of injection volumes of FlextdTomato did not impact expression, we sought to compare the transfection rate of viral injections to that of double transgenic reporter mice. To create the double transgenic mice, Gad2-Cre mice were crossed with LSL-tdTomato mice. Hybridization chain reaction (HCR) in situ hybridization staining showed that the two methods expressed tdTomato at similar rates. The median double transferior transfection rate of  $89\ \%$ was similar to the median viral injection transfection rate of 88 % and no statistical difference was found (p = .52). Both the double transgenic and the viral transfection rates were comparable to the accuracy of HCR probes, ~80-85 %, which provided evidence that the majority of GABAergic cells express tdTomato (Choi et al., 2018). HCR in situ hybridization does not label all GABAergic cells because mRNAs are transient and a detectable amount of hybridization must occur. Due to the uncertainty in the completeness of HCR in situ hybridization labeling, the percentage of tdTomato cells expressing GABA could not be directly quantified. tdTomato could be expressed in non-GABAergic cells if the Cre-Lox system were leaky or had germline recombination. Outside of tamoxifen-inducible systems, minimal leak has been reported (Stifter and Greter, 2020). Germline recombination results in major changes in fluorescent reporter expression, though the observed expression patterns match prior descriptions of GABAergic neurons in the cortex (Douglas and Martin, 2017; Song and Palmiter, 2018). Since neither of these potential pitfalls is likely, we concluded that cells expressing tdTomato are GABAergic.

# 2.3. The experimental design to compare the expression of multiple fluorescent proteins

After establishing parameters for expressing a single fluorophore, we investigated two methods of introducing multiple fluorophores. In the single-virus method, one virus is injected into a double transgenic

reporter mouse, while in the double-virus method, a mixture of two viruses is injected into a Cre driver mouse. In our experiments, tdTomato was expressed in the Cre-producing neuronal subpopulation while GCaMP, being under the Synapsin promoter, targeted all neurons (Fig. 2). We next quantified the performance of the single- and double-virus methods.

# 2.4. The double-virus method has higher coexpression than the single-virus method in Gad2 mouse somatosensory cortex

To determine whether the single-virus method or the double-virus method optimally expresses multiple fluorophores, we quantified the coexpression for both methods *in vitro*. Only neurons expressing tdTo-mato were considered for quantification because all tdTomato positive cells should express GCaMP, while only a fraction of the GCaMP positive cells should express tdTomato. The double-virus method resulted in a significantly higher (p < .0001) percentage of neurons coexpressing tdTomato and GCaMP. Samples in the single-virus method group had a median coexpression of 14 %, while samples in the double-virus method group had a median coexpression of 55 % (Fig. 3a).

Dual-color imaging is dependent on fluorophore coexpression because both fluorophores must be present in order to classify a cell in the subpopulation of interest and to record its activity. Dual-color imaging with minimal coexpression provides only population activity data, which could be done with single color imaging. Low coexpression in the single-virus method group thus eliminates the information gained by including a cell-type-specific fluorophore. Alternatively, the double-virus method shows high coexpression, allowing for subpopulation identification and, when used *in vivo*, collection of population activity data.

# 2.5. The double-virus method results in higher coexpression across mouse lines and brain regions

After a disparity in coexpression was observed in Gad2 mouse cortex, other mouse lines and brain regions were investigated. The double-virus method resulted in higher coexpression in PV mouse cortex with 19 % coexpression, while the single-virus method averaged 13 % coexpression (Fig. 4a). Gad2 mouse hippocampus also showed higher coexpression using the double-virus method, which averaged 28 % compared to 15 %

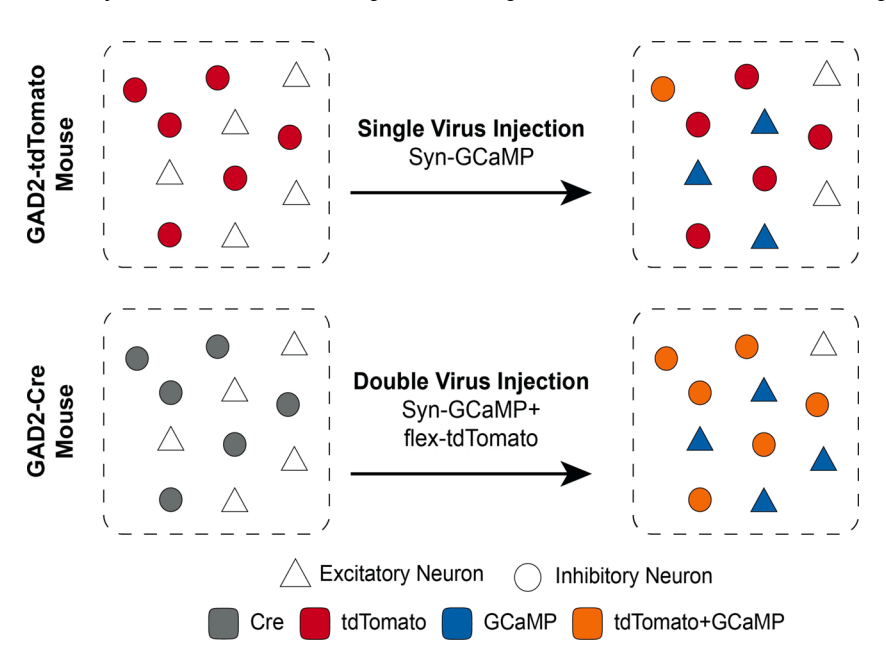


Fig. 2. Schematic of the single-virus and double-virus methods. In the single-virus method, a double transgenic reporter mouse expressing tdTomato in the cell type of interest is injected with Syn-GCaMP virus. In the double-virus method, a Cre driver mouse is injected with both Flex-tdTomato and Syn-GCaMP viruses.

# **Expression in Gad2-Cre Mouse Somatosensory Cortex**

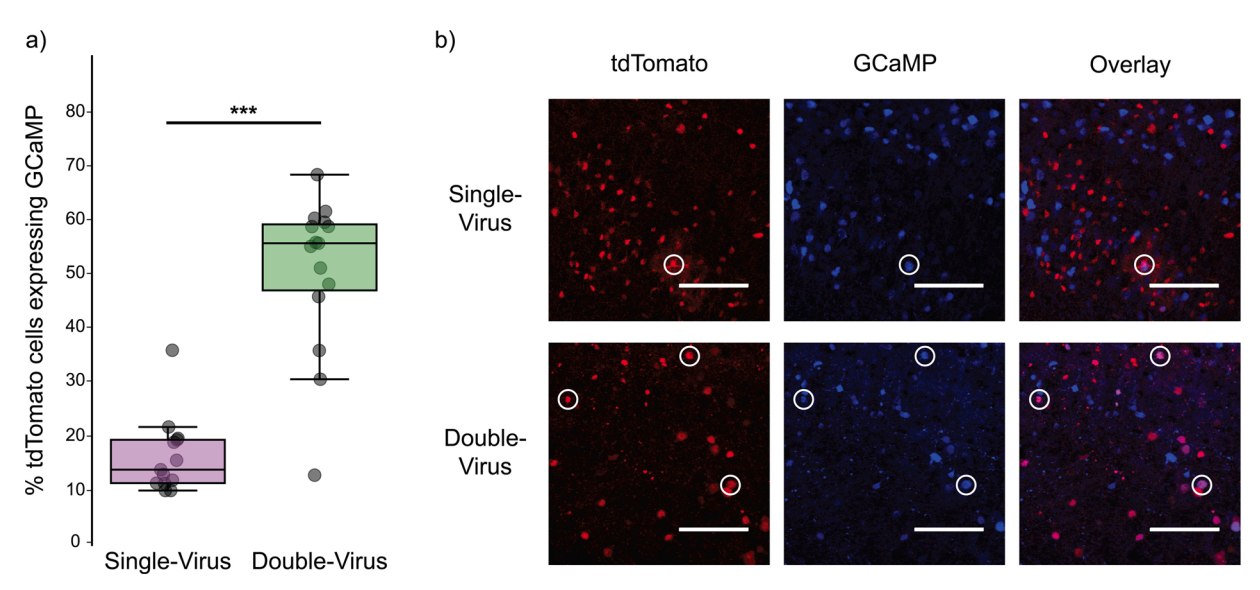


Fig. 3. In vitro comparison of coexpression in the somatosensory cortex of Gad2-Cre mice. (a) The double-virus method resulted in significantly more overlap than the single-virus method (n=13 and 15 slices for the single-virus and double-virus methods, respectively. p<.0001, Wilcoxon Rank Sum Test). (b) Representative images of the single-virus and the double-virus methods. Circles indicate neurons expressing both GCaMP and tdTomato. Scale bars:  $100 \mu m$ .

for the single-virus method (Fig. 4c). The difference in coexpression for both sample groups reached statistical significance (p < .05). CaMKII-Cre mice also showed more coexpression using the double-virus method than the single-virus method. Due to the high density of CaM-KII positive cells in the cortex, individual cells could not be reliably identified for quantification (data not shown). Investigation of additional variables such as the fluorescent proteins expressed and the AAV serotype are left to future studies, though we would expect results consistent with our findings.

## 2.6. The double-virus method results in higher coexpression in vivo

After establishing that the double-virus method resulted in better coexpression in vitro, we investigated the functionality in vivo. Both the single-virus method and the double-virus method were used to observe awake spontaneous activity in layer 2/3 somatosensory cortex. Cells without at least one calcium event were excluded from analysis because cells only expressing tdTomato cannot be distinguished from inactive cells expressing both tdTomato and GCaMP. The percent of active, GCaMP positive neurons expressing tdTomato was significantly higher when using the double-virus method. The single-virus method had a median coexpression of 1 % while the double-virus method had a median coexpression of 9 % (Fig. 5a). Sample traces were shown from cells expressing only GCaMP and from cells coexpressing GCaMP and tdTomato (Fig. 5b). Traces from cells exclusively expressing tdTomato were not shown because tdTomato is a static fluorophore and thus the fluorescence trace does not change over time. These data align with the in vitro results and confirm that the double-virus method should be used when expressing multiple fluorophores.

# 2.7. Determination of excitatory and inhibitory neurons using the double-virus method

Using the data from the double-virus method group, we investigated whether neurons could be classified as excitatory or inhibitory. In order to discriminate excitatory and inhibitory neurons, tdTomato positive cells must be GABAergic and tdTomato negative cells must be non-GABAergic. As discussed previously, all of the tdTomato expressing cells are GABAergic because the Cre-Lox system has very low leak levels.

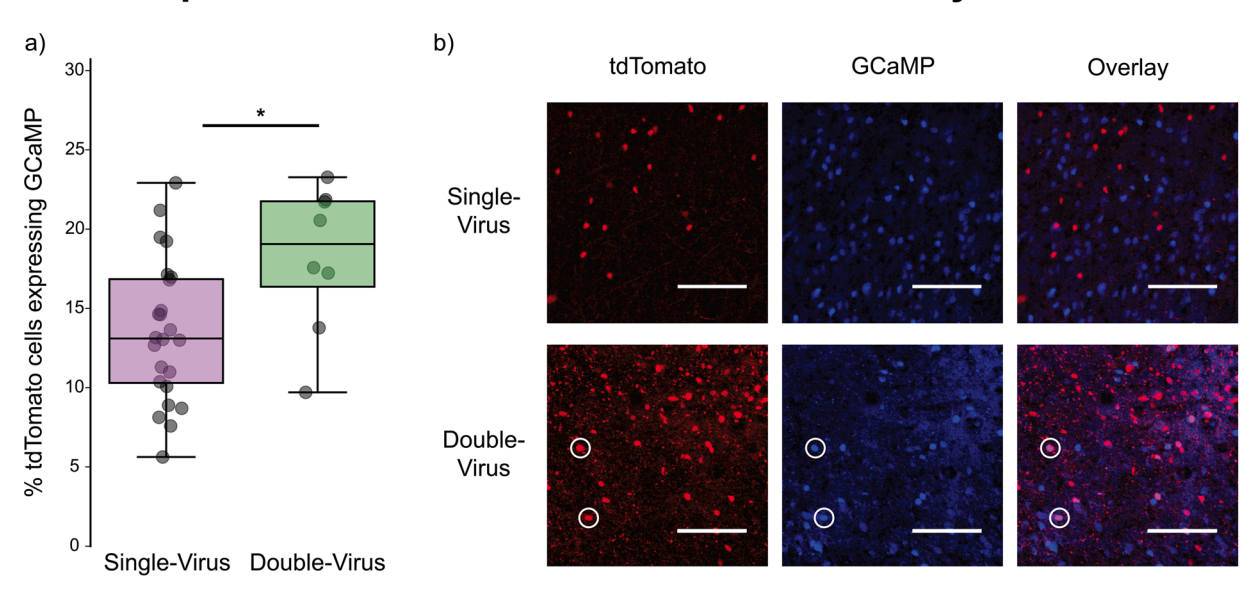
Next,  $\sim\!10$  % of GCaMP positive cells expressed tdTomato, which is comparable but below the 15–20 % of neurons reported to be GABAergic in layer 2/3 somatosensory cortex (Tremblay et al., 2016). Because the observed range of tdTomato-positive cells was below the reported literature value, some GABAergic cells may not express tdTomato and would then be erroneously classified as excitatory. Due to the high number of excitatory neurons relative to the number of GABAergic neurons, this small number of misclassifications should not impact population level conclusions. Consequently, cells expressing tdTomato were labeled as inhibitory and cells not expressing tdTomato were labeled as excitatory. These data demonstrate one example of the additional functionality provided by dual-color imaging using the double-virus method.

### 3. Discussion

As experiments increasingly incorporate multiple fluorescent proteins, determining the optimal expression method will allow for more robust characterization of activity in specific cell types. Here we established the double-virus method as the optimal method for introducing multiple fluorescent proteins. Higher coexpression using the double-virus method occurred in multiple brain regions and across mouse lines. When using one static and one dynamic fluorophore, expressing both fluorophores from viruses enabled activity data to be collected from a greater number of cells in the population of interest. Physiological measures of activity and coexpression *in vivo* confirmed the *in vitro* results. Using the double-virus method, coexpression was robust enough that cells could be classified as inhibitory or excitatory based on whether the cell did or did not express tdTomato, respectively. The double-virus method is significantly more effective than the single-virus method for simultaneously collecting population and cell-type-specific activity.

The single-virus method expresses the two fluorophores in distinct sets of cells, though, in contrast to the double-virus method, both fluorophores were rarely observed in the same cell. We believe the lack of coexpression in the single-virus method stems from asymmetric access to cellular resources between fluorophores. Robust fluorophore expression in separate cells verifies viral expression in double transgenic mice, thus narrowing the potential mechanisms causing low coexpression to those involved in producing detectable levels of multiple

# **Expression in PV-Cre Mouse Somatosensory Cortex**



# **Expression in Gad2-Cre Mouse Hippocampus**

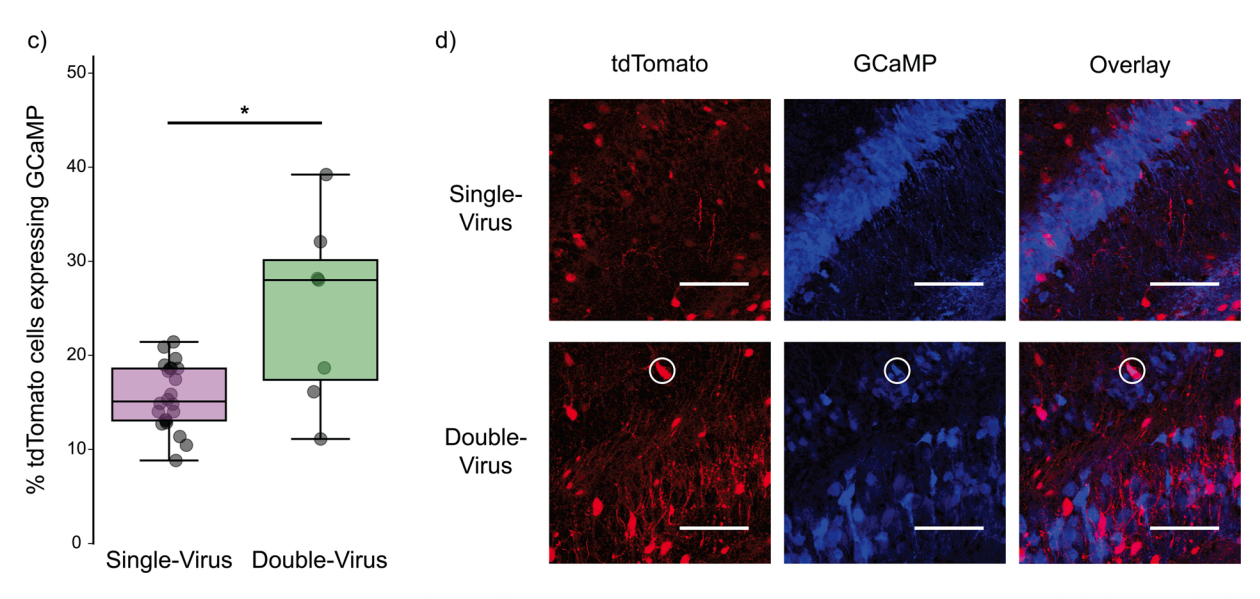


Fig. 4. In vitro comparison of coexpression across mouse lines and brain regions. (a) In PV mouse cortex, coexpression is significantly higher using the double-virus method than the single-virus method (n = 24 and 8 slices for the single- and double-virus methods, respectively. p < .05, Wilcoxon Rank Sum Test). (b) Representative images of PV mouse cortex. Circles indicate neurons expressing both GCaMP and tdTomato. Scale bars: 100  $\mu$ m. (c) Gad2 mouse hippocampus showed significantly higher coexpression using the double-virus method than the single-virus method (n = 22 and 7 for the single- and double-virus methods, respectively. p < .05, Wilcoxon Rank Sum Test). (d) Representative images of Gad2 mouse hippocampus. Circles indicate neurons expressing both GCaMP and tdTomato. Scale bars: p < .05, Wilcoxon Rank Sum Test).

fluorescent proteins in the same cell. Cells have a limited capacity to produce and store proteins (Li et al., 2014; Kintaka et al., 2016), and when this threshold is approached additional proteins are not expressed (Buttgereit and Brand, 1995; Shah et al., 2013; Qian et al., 2017). Double transgenic reporter mice express cell-type-specific fluorescent proteins as juveniles (López-Bendito et al., 2004; Besser et al., 2015), resulting in mature mice containing high fluorophore levels prior to the viral injection. Strong transgenic fluorophore expression occupies protein production capacity, which subsequently reduces the translation of additional fluorophores in the subpopulation of interest. Viral expression is then limited to cells outside the subpopulation of interest. With at most one fluorophore produced per cell, both fluorophores are observed

in the samples but coexpression is minimal. Because transgenic fluorophore expression and viral fluorophore expression have inherently different time courses, any combination of reporter mouse and viral injection will have low coexpression, regardless of the mouse line or the AAV serotype. To directly test the impact of asynchronous fluorophore production on coexpression, two viruses could be injected at different points in time with varying intervals between the injections. We predict that longer intervals would increase resource asymmetry, resulting in reduced coexpression.

In contrast to the single-virus method, the double-virus method introduces both fluorophores simultaneously. Ideally the fluorophores would express independently of each other, though the observed

# Expression in Gad2-Cre Mouse Cortex in vivo

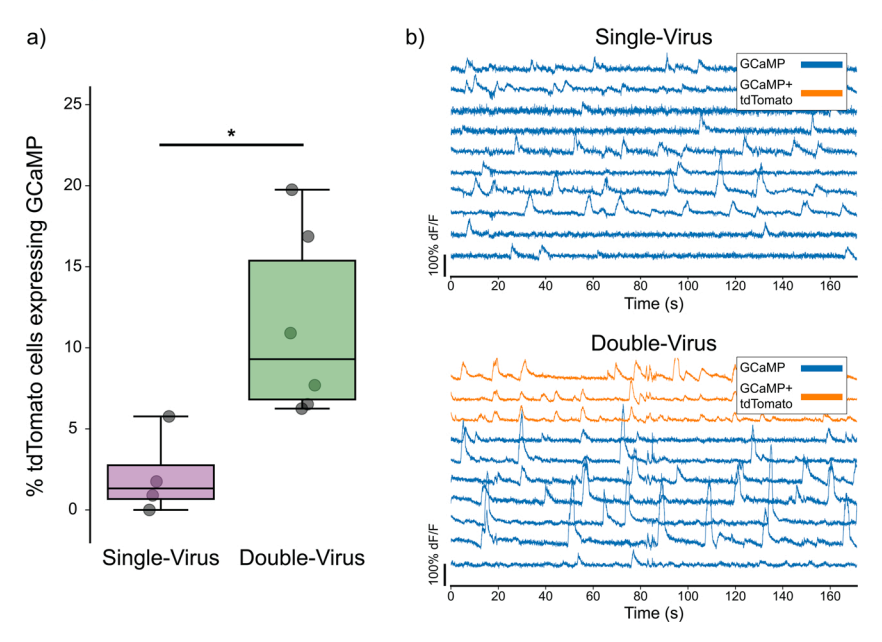


Fig. 5. In vivo comparison of coexpression in the somatosensory cortex of Gad2-Cre mice. (a) The percent of GCaMP neurons expressing tdTomato is significantly higher using the double-virus method than using the single-virus method (n = 4 and 6 mice for the single- and double-virus methods, respectively.  $p<.05,\,$  Wilcoxon Rank Sum Test). (b) Representative traces from both tdTomato positive and tdTomato negative neurons show characteristic calcium events. Because of low coexpression, our single-virus method data set included no well-imaged calcium traces from tdTomato-positive cells.

coexpression indicates that negative effects between fluorophores exist. The literature reports that 15–20 % of GCaMP positive cells should have expressed both fluorophores (Tremblay et al., 2016), but when using the double-virus method *in vivo*, only 8–12 % of cells were identified as such (Fig. 5a). The lower coexpression is likely caused by variability in viral transfection among the cells, which is unavoidable with a bolus injection. Some cells receive a high amount of one virus, which causes high expression of the corresponding fluorophore (Cohen and Kobiler, 2016). As demonstrated previously, strong fluorophore expression consumes cellular resources, thus impairing production of a second fluorophore. Despite lower fidelity when incorporating multiple fluorophores, expression with the double-virus method remains high enough to record population activity and identify the subpopulation of interest.

Beyond calcium imaging in two identified neural populations, the double-virus method described here would be useful for other experiments involving multiple genetically encoded proteins. Here, we highlight two additional applications: voltage imaging and the study of engrams. Voltage imaging resolves sub-threshold membrane fluctuations, which provide insight into the internal state of the cell (Hochbaum et al., 2014; Gong et al., 2015; Abdelfattah et al., 2019; Piatkevich et al., 2019). When combined with a static cell-type-specific marker, voltage indicators could elucidate the effect of population activity on the internal state of cells in the subpopulation of interest. Subsequently, these data would also illuminate how millivolt fluctuations in specific cell types impact network dynamics and animal behavior. To further understand the role of individual cell types, dual-color imaging could be incorporated in engram studies. An engram is a physical memory trace distributed throughout the brain (Liu et al., 2012; Roy et al., 2019). Engram experiments traditionally involve behavior and histology (Liu et al., 2014; Kitamura et al., 2017; Josselyn and Tonegawa, 2020), though imaging has become increasingly prevalent as head-fixed setups incorporate more behavioral accommodations (Milczarek et al., 2018; Ghandour et al., 2019). Dual-color imaging provides the multi-faceted information necessary to explore the relationship between cell types and memory traces. In fact, one group already used dual-color imaging to investigate the role of PV cells in engram formation across hippocampal subregions (Hainmueller and Bartos, 2018). Voltage imaging and engram investigation represent just a few of the many experimental areas which could incorporate dual-color imaging and the double-virus method. As imaging technologies continue to advance,

opportunities to utilize multiple fluorophores will emerge.

#### 4. Methods

## 4.1. Ethics

All experimental protocols were approved by the Boston University Institutional Animal Care and Use Committee.

### 4.2. Surgeries

Mice were induced with 3.0 % isoflurane, then anesthesia was reduced throughout surgery. The mouse's body temperature was maintained at 37 °C throughout the surgery using a temperature monitored heating pad. The mouse's eyes had ointment applied to prevent drying. Mice used for in vitro experiments had a borehole drilled, while mice that were imaged in vivo had a cranial opening (3 mm in diameter) drilled above the somatosensory cortex. Viruses were injected according to the viral injection procedure described in Section 4.3 and left to diffuse throughout the tissue for 10 min before the syringe was withdrawn. For in vivo imaging mice, a 1 mm aluminum cannula with a glass coverslip attached was placed above the brain and dental cement was used to secure the window. A custom headbar was attached to the skull and the remainder of the exposed skull was covered with dental cement. When applicable, the window was covered with tape to prevent debris from entering. Mice received analgesia Buprenorphine (0.1-0.2 mg/kg) post-surgery every 12 h for 48 h.

## 4.3. Viral injections

Mice between two to six months of either gender were used for experiments. The single-virus method used Gad2-Cre mice (The Jackson Laboratory, stock #028867) or PV-Cre mice (The Jackson Laboratory, stock #017320) with a C57BL/6 J background crossed with lox-stop-lox tdTomato reporter mice (The Jackson Laboratory, stock #007914). Mice were injected with 600 nl AAV9.Syn.jGCaMP7f.WPRE. The double-virus method used Gad2-Cre mice (The Jackson Laboratory, stock #028867) or PV-Cre mice (The Jackson Laboratory, stock #017320) with a C57BL/6 J background injected with 600 nl AAV9.Syn.jGCaMP7f.WPRE and 200 nl AAV9.FLEX.tdTomato. Viral titer experiments used Gad2-Cre

mice specified previously injected with 100–300 nl of AAV9.FLEX. tdTomato. Injections were placed stereotaxically at 1.4 mm posterior, +/- 2 mm medial, and 500  $\mu m$  below Bregma for cortical experiments and 2 mm posterior, +/- 1.4 mm medial, and 1.6 mm below Bregma for hippocampal experiments. A 10  $\mu l$  syringe (World Precision Instruments) with a 33-gauge needle (NF33BL; World Precision Instruments) injected at 50 nl/min for the somatosensory hip experiments and 100 nl/min for hippocampal experiments controlled by a microsyringe pump (UltraMicroPump 3–4; World Precision Instruments).

# 4.4. Transcardial perfusion and slicing

Three to six weeks post surgery, animals were sacrificed via transcardial perfusion. Mice were anesthetized and .1 ml of Euthasol was administered via intraperitoneal injection. When the mouse could no longer feel pain, cold phosphate buffered saline (PBS) and then 4% paraformaldehyde (Thermo Fisher Scientific) were transcardially perfused through the mouse. The brain was extracted and kept in 4% paraformaldehyde overnight before being transferred to PBS. 50  $\mu m$  coronal slices were obtained between -1 mm and -2 mm posterior from Bregma for somatosensory cortex experiments and between -1.5 mm and -2.5 mm posterior from Bregma for hippocampal experiments.

# 4.5. Hybridization chain reaction in situ hybridization

All reagents were purchased from Molecular Instruments. Samples were pre-hybridized in probe hybridization buffer for 30 min. Samples were then incubated in the probe solution overnight at 37 °C. Samples were transferred to amplification buffer and left at room temperature for 30 min. Hairpins for Gad2 were snap cooled by heating them to 95 °C for 90 s and cooling them at room temperature for 30 min. Samples were then transferred from the amplification buffer to the hairpin solution, which was left at room temperature overnight. Samples were successively transferred to solutions of 25 %, 50 %, 75 %, and 100 % SCCT (saline-sodium citrate buffer with Triton X) in probe solution for 10 min each at room temperature. Throughout all steps, samples were covered in foil. Prior to imaging, samples were stored at 4 °C.

# 4.6. Immunohistochemical staining and confocal imaging

Slices were blocked in with 5 % normal goat serum (Thermo Fisher Scientific) and 95 % PBST (PBS with .2 % v/v Triton X) for 1 h. Slices were then transferred to wells containing primary antibody (1:1000 rabbit anti GFP:PBST (Thermo Fisher Scientific)) and left at 4  $^{\circ}\text{C}$  for 24 h. Slices were washed three times for 10 min in PBST. They were then transferred to wells containing secondary antibody (1:500 Alexa 488 goat anti-rabbit:PBST, Thermo Fisher Scientific) and left in the dark for 2 h. Slices were mounted on slides using Vectashield (Vector Laboratories) and sealed with a coverslip. Slides were left to dry for at least one day prior to imaging. Imaging was conducted on an Olympus FV3000 microscope using a 20x air objective. Z stacks with 5  $\mu m$  step size were acquired starting at the bottom of the tissue and ending at the top of the tissue.

## 4.7. Two photon in vivo imaging

Mice were handled for 10 min per day for 3 days prior to imaging to reduce stress associated with head fixation. Mice were then head fixed to a custom aluminum frame and placed on a low-friction treadmill to allow the mouse to run freely during imaging. A dark and quiet imaging environment was maintained throughout imaging. Thorlabs software controlled a mode locked Ti:Sapphire laser (Chameleon Ultra II; Coherent) which was used to image the mice at wavelengths between 900 and 920 nm. Two photo-multiplier tubes (Hamamatsu) with red and green filters were used to simultaneously collect the respective wavelength activation. Images were obtained using a 16x, .8 numerical

aperture water immersion objective at 29.2 frames per second with a field of view of  $500 \times 500$  µm. Imaging sessions were 5000 frames long.

### 4.8. Image analysis

Confocal image analysis was completed using ImageJ and the open source CellCounting package (https://github.com/ZachPenn/CellCounting). ImageJ was used to project the Z stacks into a single plane based on the image standard deviations throughout the stack. Images were then transferred to the CellCounting software, where the provided scripts were modified and the parameters were fit to each image set. Only regions containing fluorescence were considered for quantification. Cells with at least 50 % overlap were considered as coexpressing both fluorophores.

Two photon image analysis was completed using a pre-published package, CaImAn (Giovannucci et al., 2019), in the Python programming language. CaImAn implements a combination of rigid motion correction to correct for brain motion as well as calcium image source separation based on constrained non-negative matrix factorization to identify regions of interest. Both spatial and temporal patterns are used to identify regions of interest. dF/F fluorescence traces were extracted from each region of interest. The green channel was used for region of interest identification and trace extraction while the red channel was used for classification of regions of interest as tdTomato-positive or -negative. To determine whether a cell expressed tdTomato, the weighted regions of interest were multiplied by the corresponding intensities in the red channel summary image. Summary images were produced by taking the mean fluorescence over time. If the resulting tdTomato intensity in the cell was more than two standard deviations above the mean fluorescence in the red channel summary image, then the cell was considered tdTomato-positive.

# Financial support

Support for this study comes from NIHR01 NS054281(to JAW) and NIH training grant at Boston University, T32 EB006359(to JFN). Research reported in this publication was supported by the Boston University Micro and Nano Imaging Facility and the Office of the Director, National Institutes of Health of the National Institutes of Health under award Number S100D024993. The content is solely the responsibility of the authors and does not necessarily represent the official views of the National Institutes of Health.

### Informed consent

Not applicable.

# **Declaration of Competing Interest**

None.

### CRediT authorship contribution statement

**Jacob F. Norman:** Conceptualization, Formal analysis, Investigation, Data curation, Writing - original draft. **Bahar Rahsepar:** Conceptualization, Methodology, Writing - review & editing. **Jad Noueihed:** Methodology, Software. **John A. White:** Project administration, Resources, Writing - review & editing, Funding acquisition.

# Acknowledgements

The authors thank Cam Condylis and the Dr. Jerry Chen Lab for technical advice and assistance. The authors also thank Dr. Fernando R. Fernandez and Dr. Allyson Sgro for help throughout the revision process.

#### References

- Abdelfattah, A.S., Kawashima, T., Singh, A., Novak, O., Liu, H., Shuai, Y., Huang, Y.C., Campagnola, L., Seeman, S.C., Yu, J., Zheng, J., Grimm, J.B., Patel, R., Friedrich, J., Mensh, B.D., Paninski, L., Macklin, J.J., Murphy, G.J., Podgorski, K., Lin, B.J., Chen, T.W., Turner, G.C., Liu, Z., Koyama, M., Svoboda, K., Ahrens, M.B., Lavis, L.D., Schreiter, E.R., 2019. Bright and photostable chemigenetic indicators for extended in vivo voltage imaging. Science (80-) 365, 699–704. https://doi.org/10.1126/science.aav6416.
- Adler, A., Zhao, R., Shin, M.E., Yasuda, R., Gan, W.B., 2019. Somatostatin-Expressing Interneurons Enable and Maintain Learning-Dependent Sequential Activation of Pyramidal Neurons. Neuron 102, 202–216. https://doi.org/10.1016/j. neuron.2019.01.036 e7.
- Benes, F.M., Berretta, S., 2001. GABAergic interneurons: implications for understanding schizophrenia and bipolar disorder. Neuropsychopharmacology 25, 1–27. https:// doi.org/10.1016/S0893-133X(01)00225-1.
- Besser, S., Sicker, M., Marx, G., Winkler, U., Eulenburg, V., Hülsmann, S., Hirrlinger, J., 2015. A transgenic mouse line expressing the red fluorescent protein tdTomato in GABAergic neurons. PLoS One 10, e0129934. https://doi.org/10.1371/journal. pope.0120934
- Buttgereit, F., Brand, M.D., 1995. A hierarchy of ATP-consuming processes in mammalian cells. Biochem. J. 312. 163–167. https://doi.org/10.1042/bi3120163.
- Choi, H.M.T., Schwarzkopf, M., Fornace, M.E., Acharya, A., Artavanis, G., Stegmaier, J., Cunha, A., Pierce, N.A., 2018. Third-generation in situ hybridization chain reaction: multiplexed, quantitative, sensitive, versatile. Robust. Dev 145. https://doi.org/ 10.1242/dev.165753.
- Cohen, E.M., Kobiler, O., 2016. Gene expression correlates with the number of herpes viral genomes initiating infection in single cells. PLoS Pathog. 12. https://doi.org/ 10.1371/journal.ppat.1006082.
- Danielson, N.B., Turi, G.F., Ladow, M., Chavlis, S., Petrantonakis, P.C., Poirazi, P., Losonczy, A., 2017. In vivo imaging of dentate gyrus mossy cells in behaving mice. Neuron 93, 552–559. https://doi.org/10.1016/j.neuron.2016.12.019 e4.
- Dougherty, J.D., Zhang, J., Feng, H., Gong, S., Heintz, N., 2012. Mouse transgenesis in a single locus with independent regulation for multiple fluorophores. PLoS One 7. https://doi.org/10.1371/journal.pone.0040511.
- Douglas, R., Martin, K., 2017. Inhibition in Cortical Circuits. n.d.. https://doi.org/ 10.1016/j.cub.2009.03.003.
- Engelhard, B., Finkelstein, J., Cox, J., Fleming, W., Jang, H.J., Koay, S.A., Thiberge, S.Y., Daw, N., Tank, D.W., 2020. Specialized coding of sensory, motor, and cognitive variables in VTA dopamine neurons. Nature 570, 509–513. https://doi.org/10.1038/s41586-019-1261-9.Specialized.
- Feil, S., Valtcheva, N., Feil, R., 2009. Inducible cre mice. Methods Mol. Biol. 530, 343–363. https://doi.org/10.1007/978-1-59745-471-1\_18.
- Ferguson, B.R., Gao, W.J., 2018. Pv interneurons: critical regulators of E/I balance for prefrontal cortex-dependent behavior and psychiatric disorders. Front. Neural Circuits. https://doi.org/10.3389/fncir.2018.00037.
- Fogaça, M.V., Duman, R.S., 2019. Cortical GABAergic dysfunction in stress and depression: new insights for therapeutic interventions. Front. Cell. Neurosci. https:// doi.org/10.3389/fncel.2019.00087.
- Gao, R., Penzes, P., 2015. Common mechanisms of excitatory and inhibitory imbalance in schizophrenia and autism Spectrum disorders. Curr. Mol. Med. 15, 146–167. https://doi.org/10.2174/1566524015666150303003028.
- Garcia-junco-clemente, P., Tring, E., Ringach, D.L., Joshua, T., Angeles, L., Angeles, L., Angeles, L., 2019. State-dependent subnetworks of parvalbumin-expressing interneurons in neocortex. Cell Rep. 26, 2282–2288. https://doi.org/10.1016/j.celrep.2019.02.005.State-Dependent.
- Ghandour, K., Ohkawa, N., Fung, C.C.A., Asai, H., Saitoh, Y., Takekawa, T., Okubo-Suzuki, R., Soya, S., Nishizono, H., Matsuo, M., Osanai, M., Sato, M., Ohkura, M., Nakai, J., Hayashi, Y., Sakurai, T., Kitamura, T., Fukai, T., Inokuchi, K., 2019. Orchestrated ensemble activities constitute a hippocampal memory engram. Nat. Commun. 10 https://doi.org/10.1038/s41467-019-10683-2.
- Giovannucci, A., Friedrich, J., Gunn, P., Kalfon, J., Brown, B.L., Koay, S.A., Taxidis, J., Najafi, F., Gauthier, J.L., Zhou, P., Khakh, B.S., Tank, D.W., Chklovskii, D.B., Pnevmatikakis, E.A., 2019. CalmAn an open source tool for scalable calcium imaging data analysis. Elife 8. https://doi.org/10.7554/eLife.38173.
- Gong, S., Doughty, M., Harbaugh, C.R., Cummins, A., Hatten, M.E., Heintz, N., Gerfen, C. R., 2007. Targeting Cre recombinase to specific neuron populations with bacterial artificial chromosome constructs. J. Neurosci. https://doi.org/10.1523/ INITIADSCI.2702.07.2007.
- Gong, Y., Huang, C., Li, J.Z., Grewe, B.F., Zhang, Y., Eismann, S., Schnitzer, M.J., 2015. High-speed recording of neural spikes in awake mice and flies with a fluorescent voltage sensor. Science (80-.) 350, 1361–1366. https://doi.org/10.1126/science. aab0810.
- Gritton, H.J., Howe, W.M., Romano, M.F., DiFeliceantonio, A.G., Kramer, M.A., Saligrama, V., Bucklin, M.E., Zemel, D., Han, X., 2019. Unique contributions of parvalbumin and cholinergic interneurons in organizing striatal networks during movement. Nat. Neurosci. 22, 586–597. https://doi.org/10.1038/s41593-019-0341-2
- Hainmueller, T., Bartos, M., 2018. Parallel emergence of stable and dynamic memory engrams in the hippocampus. Nature 558, 292–296. https://doi.org/10.1038/ s41586-018-0191-2.
- Hayashi, A., Yoshida, T., Ohki, K., 2018. Cell type specific representation of vibro-tactile stimuli in the mouse primary somatosensory cortex. Front. Neural Circuits 12. https://doi.org/10.3389/fncir.2018.00109.

- Hertäg, L., Sprekeler, H., 2019. Amplifying the redistribution of somato-dendritic inhibition by the interplay of three interneuron types. PLoS Comput. Biol. 15, e1006999 https://doi.org/10.1371/journal.pcbi.1006999.
- Hnasko, T.S., Hjelmstad, G.O., Fields, H.L., Edwards, R.H., 2012. Ventral tegmental area glutamate neurons: electrophysiological properties and projections. J. Neurosci. 32, 15076–15085. https://doi.org/10.1523/JNEUROSCI.3128-12.2012.
- Hochbaum, D.R., Zhao, Y., Farhi, S.L., Klapoetke, N., Werley, C.A., Kapoor, V., Zou, P., Kralj, J.M., MacLaurin, D., Smedemark-Margulies, N., Saulnier, J.L., Boulting, G.L., Straub, C., Cho, Y.K., Melkonian, M., Wong, G.K.S., Harrison, D.J., Murthy, V.N., Sabatini, B.L., Boyden, E.S., Campbell, R.E., Cohen, A.E., 2014. All-optical electrophysiology in mammalian neurons using engineered microbial rhodopsins. Nat. Methods 11, 825–833. https://doi.org/10.1038/NMETH.3000.
- Ishibashi, M., Egawa, K., Fukuda, A., 2019. Diverse actions of astrocytes in GABAergic signaling. Int. J. Mol. Sci. https://doi.org/10.3390/ijms20122964.
- Ittner, L.M., Götz, J., 2007. Pronuclear injection for the production of transgenic mice. Nat. Protoc. 2, 1206–1215. https://doi.org/10.1038/nprot.2007.145.
- Josselyn, S.A., Tonegawa, S., 2020. Memory engrams: recalling the past and imagining the future. Science (80-.). https://doi.org/10.1126/science.aaw4325.
- Kintaka, R., Makanae, K., Moriya, H., 2016. Cellular growth defects triggered by an overload of protein localization processes. Sci. Rep. 6, 1–11. https://doi.org/ 10.1038/srep31774.
- Kitamura, T., Pignatelli, M., Suh, J., Kohara, K., Yoshiki, A., Abe, K., Tonegawa, S., 2014. Island cells control temporal association memory. Science (80-.) 343, 896–901. https://doi.org/10.1126/science.1244634.
- Kitamura, T., Sun, C., Martin, J., Kitch, L.J., Schnitzer, M.J., Tonegawa, S., 2015. Entorhinal cortical ocean cells encode specific contexts and drive context-specific fear memory. Neuron 87, 1317–1331. https://doi.org/10.1016/j. neuron.2015.08.036.
- Kitamura, T., Ogawa, S.K., Roy, D.S., Okuyama, T., Morrissey, M.D., Smith, L.M., Redondo, R.L., Tonegawa, S., 2017. Engrams and circuits crucial for systems consolidation of a memory. Science (80-.) 356, 73–78. https://doi.org/10.1126/ science.aam6808.
- Li, G.W., Burkhardt, D., Gross, C., Weissman, J.S., 2014. Quantifying absolute protein synthesis rates reveals principles underlying allocation of cellular resources. Cell 157. 624–635. https://doi.org/10.1016/j.cell.2014.02.033.
- Liu, X., Ramirez, S., Pang, P.T., Puryear, C.B., Govindarajan, A., Deisseroth, K., Tonegawa, S., 2012. Optogenetic stimulation of a hippocampal engram activates fear memory recall. Nature. https://doi.org/10.1038/nature11028.
- Liu, X., Ramirez, S., Tonegawa, S., 2014. Inception of a false memory by optogenetic manipulation of a hippocampal memory engram. Philos. Trans. R. Soc. B Biol. Sci. https://doi.org/10.1098/rstb.2013.0142.
- López-Bendito, G., Sturgess, K., Erdélyi, F., Szabó, G., Molnár, Z., Paulsen, O., 2004.
  Preferential origin and layer destination of GAD65-GFP cortical interneurons. Cereb.
  Cortex 14, 1122–1133. https://doi.org/10.1093/cercor/bhh072.
- Luo, L., Callaway, E.M., Svoboda, K., 2018. Genetic dissection of neural circuits: a decade of progress. Neuron. https://doi.org/10.1016/j.neuron.2018.03.040.
- Marvin, J.S., Borghuis, B.G., Tian, L., Cichon, J., Harnett, M.T., Akerboom, J., Gordus, A., Renninger, S.L., Chen, T.W., Bargmann, C.L., Orger, M.B., Schreiter, E.R., Demb, J.B., Gan, W.B., Hires, S.A., Looger, L.L., 2013. An optimized fluorescent probe for visualizing glutamate neurotransmission. Nat. Methods 10, 162–170. https://doi.org/10.1038/nmeth.2333.
- Milczarek, M.M., Vann, S.D., Sengpiel, F., 2018. Spatial memory Engram in the mouse retrosplenial cortex. Curr. Biol. 28, 1975–1980. https://doi.org/10.1016/j. cub.2018.05.002 e6.
- Najafi, F., Elsayed, G.F., Cao, R., Pnevmatikakis, E., Latham, P.E., Cunningham, J.P., Churchland, A.K., 2020. Excitatory and inhibitory subnetworks are equally selective during decision-making and emerge simultaneously during learning. Neuron 105, 165–179. https://doi.org/10.1016/j.neuron.2019.09.045 e8.
- Peron, S.P., Freeman, J., Iyer, V., Guo, C., Svoboda, K., 2015. A cellular resolution map of barrel cortex activity during tactile behavior. Neuron 86, 783–799. https://doi.org/ 10.1016/j.neuron.2015.03.027.
- Piatkevich, K.D., Bensussen, S., Tseng, Han, Shroff, S.N., Lopez-Huerta, V.G., Park, D., Jung, E.E., Shemesh, O.A., Straub, C., Gritton, H.J., Romano, M.F., Costa, E., Sabatini, B.L., Fu, Z., Boyden, E.S., Han, X., 2019. Population imaging of neural activity in awake behaving mice. Nature 574, 413–417. https://doi.org/10.1038/s41586.019.1641.1
- Qian, Y., Huang, H.H., Jiménez, J.I., Del Vecchio, D., 2017. Resource competition shapes the response of genetic circuits. ACS Synth. Biol. 6, 1263–1272. https://doi.org/ 10.1021/acssynbio.6b00361.
- Roy, D., Park, Y.-G., Ogawa, S., Cho, J., Choi, H., Kamensky, L., Martin, J., Chung, K., Tonegawa, S., 2019. Brain-wide mapping of contextual fear memory engram ensembles supports the dispersed engram complex hypothesis. Brain-wide Mapp. Context., 668483 https://doi.org/10.1101/668483 fear Mem. engram ensembles Support. dispersed engram complex hypothesis.
- Sauer, B., 1998. Inducible gene targeting in mice using the Cre/lox system. Methods A Companion Methods Enzymol. 14, 381–392. https://doi.org/10.1006/ meth.1998.0593.
- Shah, P., Ding, Y., Niemczyk, M., Kudla, G., Plotkin, J.B., 2013. Rate-limiting steps in yeast protein translation. Cell 153, 1589. https://doi.org/10.1016/j. cell 2013.05.049
- Song, A.J., Palmiter, R.D., 2018. Detecting and avoiding problems when using the cre–lox system. Trends Genet. https://doi.org/10.1016/j.tig.2017.12.008.
- Stifter, S.A., Greter, M., 2020. STOP floxing around: specificity and leakiness of inducible Cre/loxP systems. Eur. J. Immunol. 50, 338–341. https://doi.org/10.1002/ eji.202048546.

- Surmeier, D.J., 2018. Determinants of dopaminergic neuron loss in Parkinson's disease. FEBS J. https://doi.org/10.1111/febs.14607.
- Swanson, O.K., Maffei, A., 2019. From hiring to firing: activation of inhibitory neurons and their recruitment in behavior. Front. Mol. Neurosci. 12, 168. https://doi.org/ 10.3389/fnmol.2019.00168.
- Tan, K.R., Yvon, C., Turiault, M., Mirzabekov, J.J., Doehner, J., Labouèbe, G., Deisseroth, K., Tye, K.M., Lüscher, C., 2012. GABA neurons of the VTA drive conditioned place aversion. Neuron 73, 1173–1183. https://doi.org/10.1016/j. neuron 2012.02.015
- Tischbirek, C.H., Birkner, A., Konnerth, A., 2017. In vivo deep two-photon imaging of neural circuits with the fluorescent Ca2+ indicator Cal-590. J. Physiol. https://doi.org/10.1113/JP272790.
- Tran, C.H., Vaiana, M., Nakuci, J., Somarowthu, A., Goff, K.M., Goldstein, N., Murthy, P., Muldoon, S.F., Goldberg, E.M., 2020. Interneuron desynchronization precedes seizures in a mouse model of Dravet syndrome. J. Neurosci. 40, 2764–2775. https://doi.org/10.1523/JNEUROSCI.2370-19.2020.
- Tremblay, R., Lee, S., Rudy, B., 2016. GABAergic interneurons in the neocortex: from cellular properties to circuits. Neuron. https://doi.org/10.1016/j.neuron.2016.06.033.
- Urban-Ciecko, J., Barth, A.L., 2016. Somatostatin-expressing neurons in cortical networks. Nat. Rev. Neurosci. 17, 401–409. https://doi.org/10.1038/nrn.2016.53.
- Zeng, H., Sanes, J.R., 2017. Neuronal cell-type classification: challenges, opportunities and the path forward. Nat. Rev. Neurosci. https://doi.org/10.1038/nrn.2017.85.